Surface plasmon-enhanced two-photon excited whispering-gallery modes ultraviolet laser from Zno microwire

Yunpeng Wang, Gangbei Zhu, Jingjing Mei, Cancan Tian, Hongzhen Liu, Fei Wang, and Dongxu Zhao

Citation: AIP Advances **7**, 115302 (2017); doi: 10.1063/1.5008768
View online: https://doi.org/10.1063/1.5008768
View Table of Contents: http://aip.scitation.org/toc/adv/7/11
Published by the American Institute of Physics

Surface plasmon-enhanced two-photon excited whispering-gallery modes ultraviolet laser from Zno microwire

Yunpeng Wang,[1] Gangbei Zhu,[2] Jingjing Mei,[1] Cancan Tian,[1] Hongzhen Liu,[1] Fei Wang,[1,a] and Dongxu Zhao[1,a]
[1]*State Key Laboratory of Luminescence and Applications, Changchun Institute of Optics, Fine Mechanics and Physics, Chinese Academy of Sciences, 3888 Dongnanhu Road, Changchun 130021, People's Republic of China*
[2]*National Key Laboratory of Shock Wave and Detonation Physics, Institute of Fluid Physics, China Academy of Engineering Physics, 621900 Mianyang, China*

(Received 9 October 2017; accepted 25 October 2017; published online 3 November 2017)

The two-photon excited UV laser with narrow line width and high Q value was obtained. The total internal reflection from the four side surfaces of the quadrilateral-ZnO microwire offered the whispering gallery mode (WGM) resonant cavity. The UV emission, resonant mechanism, and laser mode characteristics were discussed in detail for this special type of micro-cavity. In addition, in order to enhance the power of the two-photon excited UV laser, the surface plasmon enhancement by the Au nanoparticles was also performed and explained well by the theory of the localized surface plasmon. https://doi.org/10.1063/1.5008768

Multi-photon pumped lasing (MPPL) has received increasing attentions due to the broad range of possible applications in wavelength up-conversion, 3D fluorescence imaging, and 3D micro-fabrication.[1–3] Unlike common second-harmonic generation, MPPL can convert lower frequency incident photons into higher frequency emission photons through multi-photon processes without the phase-matching requirements. MPPL has been observed in organic dyes, ZnSe nanowires, and ZnO nanorods. The research of ZnO micro UV laser has attracted wide attentions, and the whispering gallery mode (WGM) laser,[4–12] is one important research directions in the field of micro-cavity quantum electrodynamics, optical fiber communication and sensor,[12,13] because of its high quality factor, high gain coefficient and lower lasing threshold. It is very easy for ZnO to form a WGM stimulated emission while the light reflects continuous in the polygon interface. Moreover, due to the small penetration depth under the one-photon excitation, non-radiative processes from surface defects will greatly affect optical properties of ZnO single crystal. In comparison, multi-photon excitation can circumvent the above limitations due to the long penetration depth.[14] Therefore, it is more saving way to use a visible laser as the excitation source to achieve MPPL rather than the deep ultraviolet laser. However, it is difficult to obtain highly efficient MPPL from ZnO nano-materials. One efficient way is enhancing the local optical field by the surface plasmons.

Surface plasmons are the interaction between the incident optical field and free electrons at the interface of metal and semiconductor, which has been used to enhance the fluorescence and Raman scattering. Also, plasmonic modulation of metal nanoparticles is a promising method for improving upconversion efficiency of rare earth phosphors.[15] However, there is no report about the surface plasmon enhanced MPPL. In this paper, we found the nano-metal surface plasmon resonance-enhanced two-photon excited WGM ultra-violet lasing in ZnO microwires.

[a]Author to whom correspondence should be addressed: wangf@ciomp.ac.cn

The ZnO microwires were prepared by the chemical vapor deposition (CVD) method with the reaction of carbon thermal reduction.[16,17] First, the mixture of the high purity ZnO powder and carbon powder was put into a mortar with the proportion of 1:1, followed by the 2 hours' grind of the mixed powder to ensure the uniformity of the mixture. Then, the mixed powder was transferred into the middle of a ceramics boat, and the ZnO seed crystals were placed on the top of the mixed powder. The ceramics boat was put inside a high temperature tube furnace, and then heated to 1000°C. The growth temperature of 1000°C was held for 40 minutes with the Ar gas flowing during the whole process. The length of the ZnO microwires are all more than 10 mm, therefore it is very easy to clip a single ZnO microwire to be tested or fabricated devices.

The morphology of the ZnO microwires are investigated by the scanning electron microscope (SEM, FESEM, Hitachi S-4800) and shown in figure 1(a), the quadrangle length D of the ZnO microwire is about 10 μm and the corner angle α equals to 60 degree as shown in figure 1(d). The cleavage facets in figure 1(a) reveals the crystal grown direction is [1$\bar{1}$00], which is in agreement with the previous work of Sohn,[18] who analyzed more details of the crystal directions in the cross-section of the quadrilateral ZnO microwire as depicted in figure 1(b). The optical axis [0001] is perpendicular to the grown direction. Figure 1(c) shows the schematic optical geometry of a quadrangle WGM cavity and the electric field direction of the WGM TE mode.[8] Only TE polarization is considered here since TM polarized emission is typically 100 times weaker, independent of the polarization of excitation.[19] The difference between this quadrilateral case and those hexagonal cases previously reported by other groups is that a part of TE polarization is corresponding to extraordinary light here because the optical axis is perpendicular to the grown direction. Figure 2(a) shows the photoluminescence spectra of the ZnO microwires excited by a He:Cd continuous laser with central wavelength of 325 nm. The spectrum consists of a narrow UV band around 400 nm and a broad green band around 550 nm. It is well known that the UV peak is originally from the near band-edge emission, while the green band is related to the defect states of oxygen vacancies,[15] which is two orders lower than the UV peak here because of the low density of the defect states.

A layer of Au nanoparticles was sputtered on the ZnO microwire by an ion sputtering apparatus, and then annealed by a high temperature furnace. The average diameter of Au nanoparticles is about

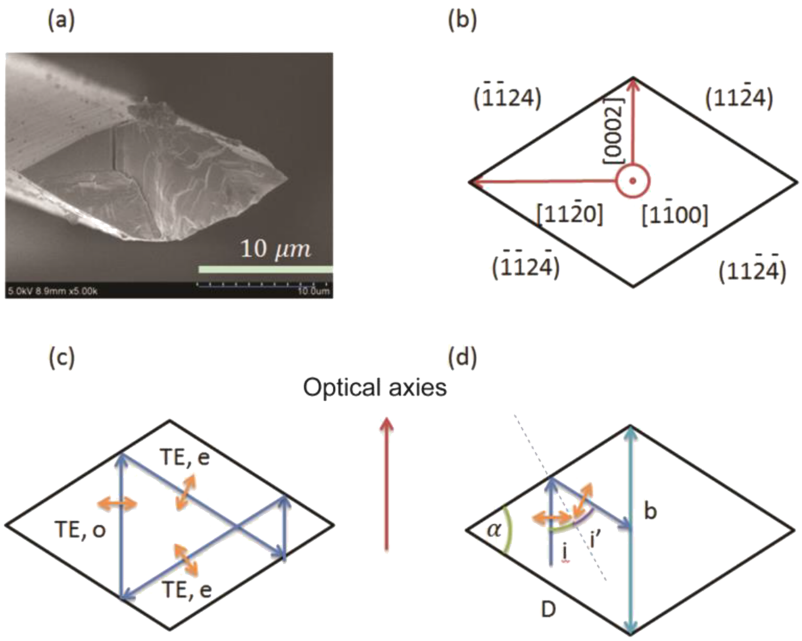

FIG. 1. (a) SEM of ZnO microwire, (b) Scheme of the cross section and crystal directions in the cross-section of the quadrilateral ZnO microwire, (c) Schematic optical geometry of a quadrilateral WGM cavity, and electric field direction of the WGM TE mode, and (d) Angles and scales in the cross section.

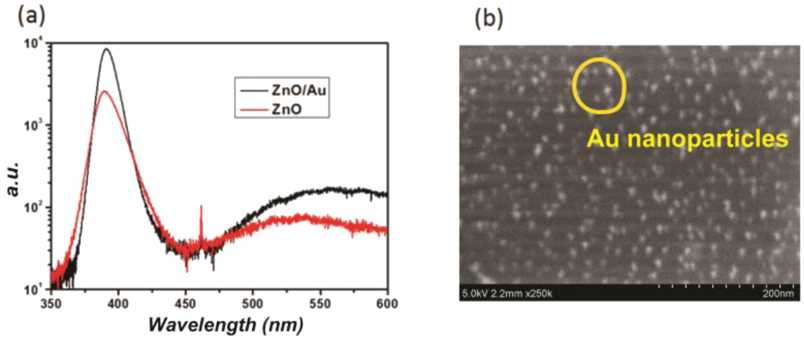

FIG. 2. (a) Photoluminescence spectra of ZnO and ZnO/Au microwires. (b) Side plane of a ZnO microwire sputtered by gold nanoparticles.

9 nm, and the average distance between two nanoparticles is about 20 nm as shown in figure 2(b). The fluorescence of Au nanoparticles modified ZnO microwire excited by the He:Cd continuous laser with central wavelength of 325 nm in figure 2(a) is several times larger than the unmodified ZnO microwire, which means its fluorescence is enhanced by the Au nanoparticles.

The ZnO microwire was adhered partly onto the long side of a glass slide horizontally with one end hung in the air.

The glass slide was placed to a sample stage with three translational degrees of freedom and two rotational ones. Three CCD cameras were set at the X, Y, Z direction of the ZnO microwire, so that the initial position recorded by the camera can be reset by adjusting the mechanical stage. The laser supplied from a Ti-sapphire femtosecond laser (Newport Company, Spitfire Ace) generated a pulse centered at 800 nm with a pulse width of 35 fs and a repetition frequency of 1 kHz. An optical parametric amplifier (OPA) (Newport Company, Topas Prime) output laser was tuned to 600 nm, passed through a neutral density filter and was focused on the ZnO microwire by a convex lens with a focal length of 50 mm. The OPA laser output was tuned to 5 mW. The luminescence from the ZnO mircowire was converged by a lens group, and was collected by a high resolution fiber spectrometer (ACTON SpectraPro 2300i).

As depicted in figure 3(a) and (b), the multi-peaks spectral structure in the range of 392 nm -398 nm reveals multiple lasing modes with the average mode spacing $\Delta\lambda$ of 0.7 nm. The spectrum is a superposition of the narrow-band laser modes and a wide-band spontaneous emission spectrum like reported in the previous work.[10] Figure 3(a) and (b) also show the emission spectra of the one ZnO microwire with Au coated and without coated, excited by a 600nm laser with different pump power. It indicates that the presence of the Au-decoration enhances lasing intensity by several folds. Figure 3(c) depicts the lasing intensity versus excitation power density, and shows that the Au decoration reduces the lasing threshold.

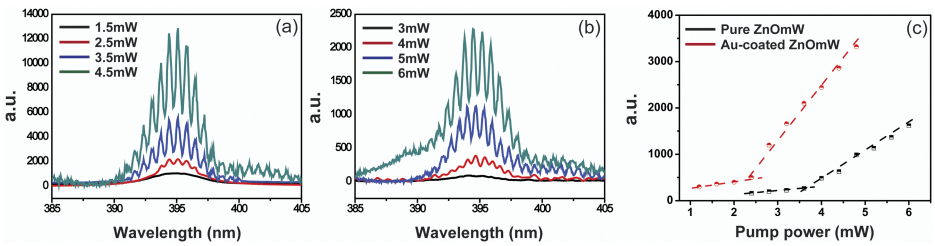

FIG. 3. (a) Emission spectra of the Au coated ZnO microwire excited by a 600nm laser with different pump power (1.5mW, 2.5mW, 3.5mW and 4.5mW). (b) Pure ZnO microwire excited by a 600nm laser with different pump power (3mW, 4mW, 5mW and 6mW). (c) The relationships between output lasing intensity and excitation power density of the ZnO (black) and ZnO/Au (red) microwire.

The enhancement of the surface plasmons can be estimated by figure 4. For the two-photon absorption process, the emission intensity is expressed by:

$$I_{out} = ASDI_{in}^2 = ASI_{in}/\beta \tag{1}$$

where A is a constant, S is the area of excitation, D=1/(βI_{in}) is the optical depth, β is the two-photon coefficient and I_{in} is the incident field intensity. It proves the linear relationship between output lasing intensity and excitation power density. As for the nanopartiles, the electric field intensity at the surface is enhanced to I_{sp}, and the emission intensity contributed from it is expressed by:

$$I'_{out} = AsdI_{sp}^2 = A\alpha S\eta I_{in}/\beta \tag{2}$$

where s is the area of nanoparticles, α=s/S is the coverage rate of nanoparticles, d=1/(βI_{sp}) is the optical depth of the enhanced electric field, and η=I_{sp}/I_{in} is the enhancement factor. Therefore, the final emission enhancement is determined by the coverage rate and the enhancement factor. Figure 2(b) shows that the coverage rate is about 10%. The enhancement factor of Au nanoparticles for the surface plasmons direction here shown in figure 4 is $(1.5|\varepsilon'/\varepsilon''|)^2$ according to the quasistatic approximation of Mie theory of the nanoparticle,[20] where ε′ and ε″ are real and imagine part of the electric constant of Au. For 600 nm excitation, this value is about 100. Therefore, the emission enhancement is about 10 folds, which agrees with the results very much.

The resonant wavelength and the corresponding mode number N can be deduced through the plane wave model for the WGM cavity:[21]

$$N = \frac{OPL}{\lambda} - 4\frac{\psi}{2\pi} \tag{3}$$

where OPL is one circulation optical path length, λ is the wavelength of the light and the respective total internal reflection phase shift:[21,22]

$$\psi = 2\tan^{-1}\left(n_0\sqrt{\frac{n_0^2-4}{3}}\right) - \pi \tag{4}$$

Since the refractivity of the reflected light (extraordinary) is different from the incident one (ordinary), the reflection angle is also different from the incident one, that is i′≠i as depicted in figure 1(d), which complicates the geometry of the optical path. For the case of the corner angle α equals to 60 degrees, one circulation optical path length here is expressed as

$$OPL = n'L_1 + n_0L_2 \tag{5}$$

$$L_1 = 2b\frac{\cos i}{\cos i'} \tag{6}$$

$$L_2 = b\left(1 + \cos(2i) - \sin(2i)\tan i'\right) \tag{7}$$

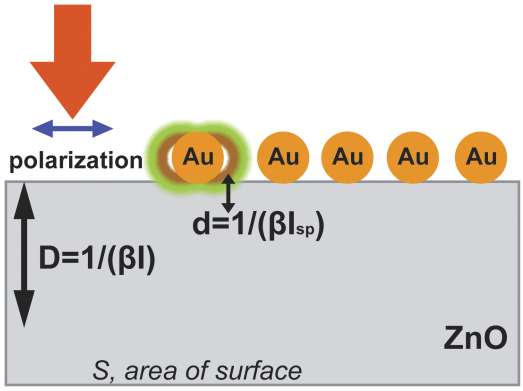

FIG. 4. Scheme of the surface plasmons enhancement with the Au nanoparticles on ZnO microwire.

where L_1 and L_2 are paths for the extraordinary and ordinary TE modes in one circulation path, respectively, i=30° is incident angle and b is the length of the shorter diagonal line, and n′ index of refractivity of the extraordinary TE modes and n′ angle of reflection derived from

$$\frac{1}{n'^2} = \frac{\cos^2(i+i')}{n_0^2} + \frac{\sin^2(i+i')}{n_e^2} \tag{8}$$

$$n' \sin i' = n_0 \sin i \tag{9}$$

into

$$n' = n_0 \frac{\sqrt{1+(1-x^2)^2 \sin^4(i) + 2\cos(2i)(1-x^2)\sin^2(i)}}{1-(1-x^2)\sin^2(i)} \tag{10}$$

$$i' = \tan^{-1}\left(\frac{1-(1-x^2)\sin^2(i)}{1+(1-x^2)\sin^2(i)} \tan i\right) \tag{11}$$

where $x=n_o/n_e$, with n_o and n_e indexes of refractivity of ordinary and extraordinary light,[21] respectively, expressed as:

$$n_0 = \left(1 + \frac{2.4885\lambda^2}{\lambda^2 - 102.3^2} + \frac{0.2150\lambda^2}{\lambda^2 - 372.60^2} + \frac{0.2550\lambda^2}{\lambda^2 - 1850^2}\right)^{1/2} \tag{12}$$

$$n_e = \left(1 + \frac{2.9535\lambda^2}{\lambda^2 - 82.30^2} + \frac{0.1660\lambda^2}{\lambda^2 - 358.60^2} + \frac{0.1050\lambda^2}{\lambda^2 - 1750^2}\right)^{1/2} \tag{13}$$

The calculation demonstrates that the nine peaks in the range 392 to 398 nm are corresponding to the mode 202 to 194 as shown in figure 5(a), with the parameter b=11.3μmb. The length b is a little larger than 9.2 μm measured form the figure 1(a), because the excitation area is at the middle of the wire while figure 1(a) is at the top the thinnest place. The theoretical peaks of WGM modes agree very well with the experimental results as depicted in figure 5(b).

It is estimated for both cases that the Q factor of this micro-cavity is about 1300 according to the equation, $Q=\lambda/\delta\lambda$, where λ and δλ are the peak wavelength and FWHM, respectively. On the other hand, the Q factor for an 4th-order polygonal cavity can be expressed as:[1]

$$Q = \frac{\pi OPLR}{\lambda(1-R^2)} \tag{14}$$

where OPL is the optical path length of one circulation, R is the reflectivity of the total internal reflection, and n is index of refractivity of the extraordinary light. The calculated OPL is in the range 77 to 79 μm for the wavelength range 392 to 398 nm. Therefore the reflectivity R=79%, which is a little smaller than the previous reported result 85% in hexagonal cross section case.[1] It is suggested that the less perfect surface condition shown in figure 1(a) results in the lower reflectivity.

The WGM laser intensity of the Au-decorated ZnO microwire is about triple as large as the uncoated ZnO microwire. The highly localized electromagnetic fields of the Au nanoparticles

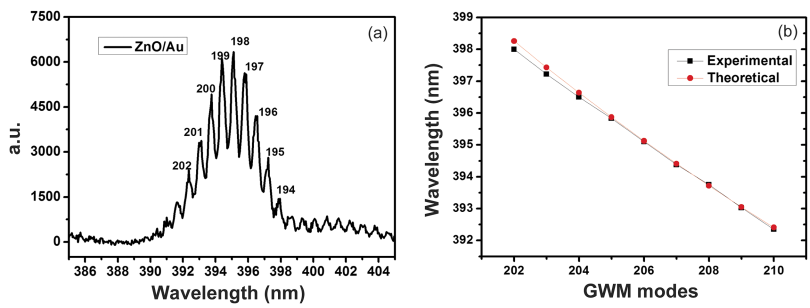

FIG. 5. (a) WGM modes of ZnO/Au microwire. (b) Experimental and theoretical results of WGM modes.

transport and manipulate the photons on sub-wavelength scales which enhance the absorption of the light. The fact that Q values for both cases are almost the same is suggested as the result of the low concentration and small scale of Au nanoparticles as shown in figure 2(b).

In summary, the two-photon excited UV laser generated in the WGM cavity, which was arose from the total internal reflection from the four side surfaces of the quadrilateral ZnO microwire, was obtained with narrow line width of 0.3 nm and high Q value of 1300. The calculated reflectivity R = 79% is due to the less perfect surface condition of the side plane. The theoretical analysis results of WGM modes agreed well with the experiment for this special type of micro-cavity. The surface plasmons enhancement by the Au nanoparticles by about 3 times was also achieved, whose results is in good agreement with the theoretical estimation. Moreover, the laser threshold is reduced from 3.6mW to 2.4mW. The results suggests that the MPPL can also be enhanced by the surface plasmons originated form the metal nanoparticles.

This work was supported by the National Natural Science Foundation of China under Grant No.11504367.

[1] G. P. Zhu, C. X. Xu, J. Zhu, C. G. Lv, and Y. P. Cui, Appl. Phys. Lett. **94**, 1 (2009).
[2] G. Xing, J. Luo, H. Li, B. Wu, X. Liu, C. H. A. Huan, H. J. Fan, and T. C. Sum, Adv. Opt. Mater. **1**, 276 (2013).
[3] C. Zhang, C. L. Zou, Y. Yan, R. Hao, F. W. Sun, Z. F. Han, Y. S. Zhao, and J. Yao, J. Am. Chem. Soc. **133**, 7276 (2011).
[4] J. Dai, C. X. Xu, Z. L. Shi, R. Ding, J. Y. Guo, Z. H. Li, B. X. Gu, and P. Wu, Opt. Mater. (Amst). **33**, 288 (2011).
[5] C. Czekalla, C. Sturm, R. Schmidt-Grund, B. Cao, M. Lorenz, and M. Grundmann, Appl. Phys. Lett. **92**, 8 (2008).
[6] G. P. Zhu, C. X. Xu, J. Zhu, C. G. Lv, and Y. P. Cui, Appl. Phys. Lett. **94**, 35 (2009).
[7] J. Dai, C. X. Xu, and X. W. Sun, Opt. Commun. **284**, 4018 (2011).
[8] J. Dai, C. X. Xu, R. Ding, K. Zheng, Z. L. Shi, C. G. Lv, and Y. P. Cui, Appl. Phys. Lett. **95**, 22 (2009).
[9] J. Dai, C. X. Xu, P. Wu, J. Y. Guo, Z. H. Li, and Z. L. Shi, Appl. Phys. Lett. **97**, 95 (2010).
[10] J. Dai, C. X. Xu, K. Zheng, C. G. Lv, and Y. P. Cui, Appl. Phys. Lett. **95**, 1 (2009).
[11] J. Dai, C. X. Xu, L. X. Sun, Z. H. Chen, J. Y. Guo, and Z. H. Li, J. Phys. D. Appl. Phys. **44**, 025404 (2010).
[12] G. Singh, A. Choudhary, D. Haranath, A. G. Joshi, N. Singh, S. Singh, and R. Pasricha, Carbon N. Y. **50**, 385 (2012).
[13] J. Yi, J. M. Lee, and W. Il Park, Sensors Actuators, B Chem. **155**, 264 (2011).
[14] T. C. He, R. Chen, W. W. Lin, F. Huang, and H. D. Sun, Appl. Phys. Lett. **99**, 1 (2011).
[15] Y. Lin, C. Xu, J. Li, G. Zhu, X. Xu, J. Dai, and B. Wang, Adv. Opt. Mater. **1**, 940 (2013).
[16] B. Zhao, M. Jiang, D. Zhao, and Y. Li, **1081**, (2015).
[17] L. Shi, F. Wang, B. Li, X. Chen, and B. Yao, **5005**, (2014).
[18] J. I. Sohn, W. Hong, S. Lee, S. Lee, J. Ku, Y. J. Park, J. Hong, S. Hwang, K. H. Park, J. H. Warner, S. Cha, and J. M. Kim **1** (2014).
[19] C. Czekalla, C. Sturm, R. Schmidt-Grund, B. Cao, M. Lorenz, and M. Grundmann, Appl. Phys. Lett. **92**, 232 (2008).
[20] S. A. Rid, O. Data, and O. Sciences, *MODERN INTRODUCTION TO SURFACE PLASMONS Theory, Mathematica Modeling and Applications* (n.d.).
[21] J. Liu, S. Lee, Y. H. Ahn, J. Y. Park, K. H. Koh, and K. H. Park, Appl. Phys. Lett. **92**, (2008).
[22] G. Jia, Optoelectron. Lett. **7**, 229 (2011).